Composites Part C: Open Access 3 (2020) 100047

Contents lists available at ScienceDirect

Composites Part C: Open Access

journal homepage: www.elsevier.com/locate/jcomc

# Flexural properties of symmetric carbon and glass fibre reinforced hybrid composite laminates

Chensong Dong

*School of Civil and Mechanical Engineering, Curtin University, GPO Box U1987, Perth, WA 6845, Australia*

ARTICLE INFO

*Keywords:*
Composite
Hybrid
Carbon
Glass
Flexural

ABSTRACT

A study on the flexural properties of symmetric carbon and glass fibre reinforced hybrid composite laminates is presented in this paper. A modelling approach was developed with the aid of Finite Element Analysis (FEA). This model was experimentally validated. With this FEA based model, various stacking sequences were studied to find the effects of hybridisation on the flexural properties. A rule of how to arrange the carbon and glass fibres in the hybrid composite was developed. It is shown that the hybrid composite has the highest flexural strength when it contains half carbon/epoxy plies and half glass/epoxy plies. Optimisation was also carried out with the objective functions being the material cost and component weight. It is shown from the optimal hybrid composite has up to half of its plies being glass/epoxy and placed on the inside of the composite.

## 1. Introduction

Carbon fibre reinforced polymer composites have been used to replace metallic components due to their light weight and high strength. However, the application of carbon fibre reinforced composites is still limited because of the high cost associated with carbon fibre. Although glass fibre possesses lower mechanical properties compared to carbon fibre, its cost is much lower than that of the carbon fibre. Thus, it may be possible to achieve desirable mechanical properties at an affordable cost via hybridisation of carbon and glass fibres [1]. Based on the hybridisation methods, hybrid composites can be categorised into intra-ply, inter-ply, sandwich and super hybrids [2,3].

A simple method for evaluating the material properties of a hybrid composite is the rule of mixtures (RoM), where the property of the hybrid composite is calculated from the properties of the virgin composites and corresponding volume concentrations. However, it has been noticed from experiments that difference exists between experimental result and the RoM prediction, and this difference is called the hybrid effect. The hybrid effect can be positive or negative depending on if the experimental result is higher or lower than the RoM prediction [4].

Previous research on carbon and glass fibre reinforced hybrid composites has shown that positive hybrid effects exist for the flexural strength [5–8]. In these studies, interply carbon fibre plies on the compressive side were replaced by glass fibre plies. Because glass fibre has higher strain-to-failure compared to carbon fibre, incorporation of glass fibre can potentially increase the strain-to-failure [9]. Dong et al. [10,11] concluded that the fibre volume fraction of the glass/epoxy section needs to be higher than that of the carbon/epoxy section in order to achieve positive hybrid effects. The replacement of carbon fibre by glass fibre on the compressive side results in asymmetric laminates. This problem can be avoided by hybrid sandwich composites. Jalalvand et al. [12] numerically studied the tensile behaviour of unidirectional carbon and glass fibre reinforced sandwich composites. The glass fibre plies were place on the outside of the hybrid composite. A damage mode domain map was derived to help design hybrid composites with the desired damage process and characteristics. Zhang et al. [13] studied the tensile, compressive and flexural behaviours of E glass and T300 carbon woven fabric reinforced hybrid sandwich composites. It was found that in order to see improvement in the tensile, compressive and flexural strength of the full glass fibre composite, the ratio of glass and carbon fibres should be 1, and the stacking sequence should be the carbon fibre plies being placed on the outside of the composite, i.e. $[C_2G_2]_S$, or the carbon and glass fibre plies being placed alternately, i.e. $[CGCG]_S$. However, it was not shown that positive hybrid effects existed.

It is shown from the literature that it is unclear if the glass fibre plies should be placed on the inside or outside of the hybrid composite for achieving the optimal stacking sequence. In this study, the flexural behaviour of symmetric carbon and glass fibre reinforced hybrid composites was studied in greater depth for identifying if any hybrid effects exist. Various fibre volume fractions of both carbon and glass fibres were studied. Optimisation was also conducted by Multi-Objective Genetic Algorithm (MOGA).

*E-mail address:* c.dong@curtin.edu.au

https://doi.org/10.1016/j.jcomc.2020.100047
Received 1 June 2020; Received in revised form 15 September 2020; Accepted 25 September 2020

**Table 1**
Constituent properties.

| Material | Tensile modulus (GPa) | Tensile strength (MPa) | Density (g/cm$^3$) | Cost ($/litre) |
|---|---|---|---|---|
| High strength carbon fibre[a] | 230 | 4900 | 1.8 | 151.2 |
| S-2 glass fibre[b] | 86.9 | 4890 | 2.46 | 103.3 |
| Epoxy[c] | 3.1 | 69.6 | 1.09 | 26.2 |

[a] T700S® 12K, Toray Industries, Inc., Tokyo, Japan
[b] Unidirectional Unitex plain weave UT-S500 fibre mat, SP System, Newport, Isle of Wight, UK
[c] Kinetix R240 high performance epoxy resin, ATL Composites Pty Ltd, Australia

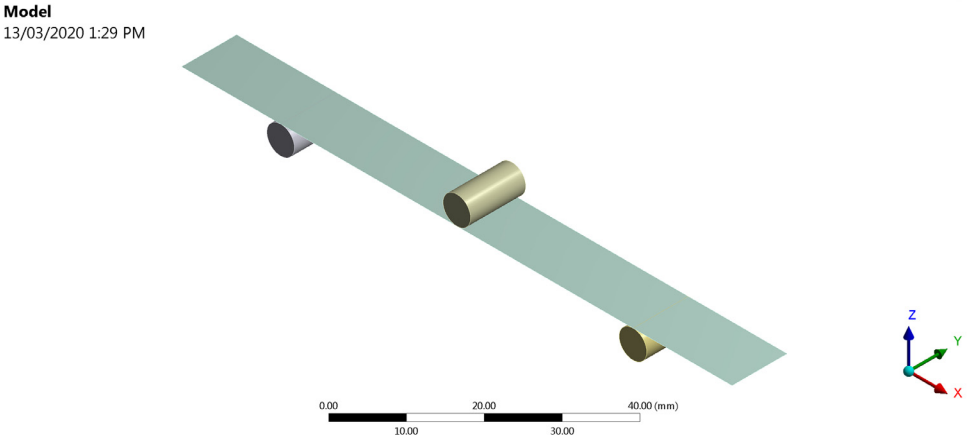


**Fig. 1.** FEA model of three point bend test.

## 2. Methodology

### 2.1. Materials

The constituent properties are summarised in Table 1 [5]. Given the constituent properties and fibre volume fraction of each lamina, the lamina properties, including the longitudinal modulus $E_{11}$ and the shear moduli $G_{12}$, $G_{13}$ and $G_{23}$, are derived by Hashin's model [14]. The transverse moduli $E_{22}$ and $E_{33}$ are derived from the stress-strain relationship [15]. The cost data are from our previous research [16].

### 2.2. Finite element analysis

In this study, three point bend test in accordance to procedure A of ASTM D7264/D7264M-15 was simulated by FEA. The FEA model was developed with the aid of Ansys ACP. The composite was modelled as a surface, as graphically shown in Fig. 1. The composite consisted of a given number of plies, and for each ply, the ply material and ply angle were defined. The calculated lamina properties were defined for each ply of the hybrid composite. Stress based failure criteria were used and five strengths: longitudinal tensile, longitudinal compressive, transverse tensile, transverse compressive and shear strengths were defined. In a three point bend test, failure commonly occurs at the compression side of the test specimen [17]. The dominant failure modes are kinking (highly localised fibre buckling [18]) and microbuckling [19]. For the microbuckling or kinking mode, Lo-Chim model [20] or Budiansky and Fleck model [21] can be used to predict the compressive strength of a unidirectional laminate. In this study, Lo-Chim model was used. This model was also used in our previous studies [5–8] for the simulation of asymmetric carbon and glass fibre reinforced hybrid composites. Lo-Chim model is given by

$$S_C = \frac{G_{12}}{1.5 + 12(6/\pi)^2\left(G_{12}/E_{11}\right)} \tag{1}$$

where $S_C$ is compressive strength, and $G_{12}$ and $E_{11}$ are shear and tensile moduli, respectively.

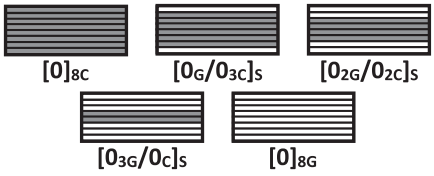


**Fig. 2.** Stacking sequences.

A pre-defined displacement was applied to the mid-span of the test specimen, and the reaction forces were obtained from the FEA results. The failure load was determined from the load-displacement curve. Because the stress distribution is uniform in compression but non-uniform in bending, from Weibull statistical theory [22], the flexural strength is about 30% higher than the compressive strength. Thus, the maximum bending load was also increased by about 30%. According to procedure A of ASTM D7264/D7264M-15, the flexural strength ($S_F$) is given by [23]:

$$S_F = \frac{3P_{\max}L}{2bh^2} \tag{2}$$

The flexural modulus ($E_F$) is given by [23]:

$$E_F = \frac{\Delta\sigma_F}{\Delta\epsilon_F} \tag{3}$$

where $L$, $b$ and $h$ are the span, width and depth of the specimen, $D$ is the maximum deflection before failure, $P_{\max}$ is the maximum load encountered before failure, and $\sigma_F$ is the flexural stress.

### 2.3. Model validation

The developed model was validated against experimental data. Five stacking sequences were chosen to be studied, as shown in Fig. 2. The test specimens consisted of eight carbon/epoxy and/or glass/epoxy plies. It was found the fibre volume fractions of the carbon/epoxy and glass/epoxy plies were 32% and 46% respectively. The thickness of specimens was around 2 mm. Three point bend test was conducted in accordance to procedure A of ASTM D7264/D7264M-15. A span-to-depth

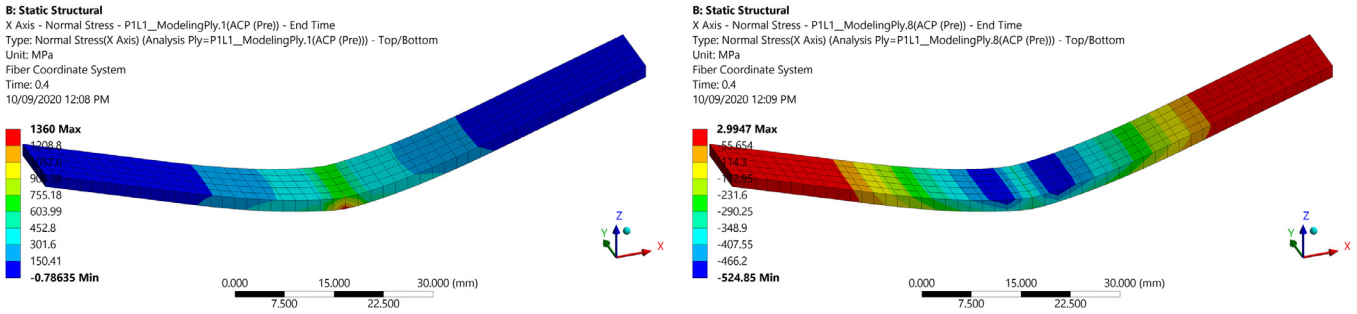


**Fig. 3.** Stresses of $[0_G/0_{3C}]_S$: Left: ply 1; right: ply 8.

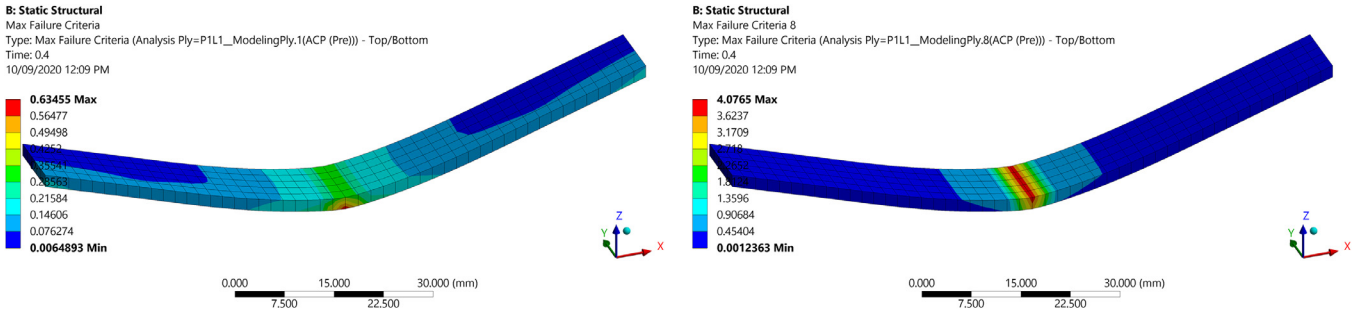


**Fig. 4.** Maximum failure criteria of $[0_G/0_{3C}]_S$: Left: ply 1; right: ply 8.

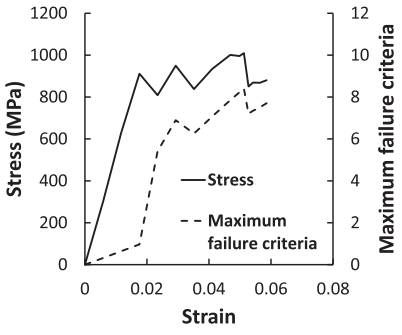


**Fig. 5.** Stress-strain curve of $[0_G/0_{3C}]_S$.

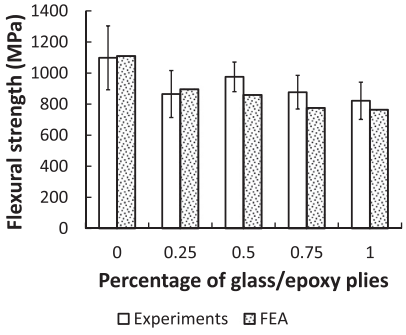


**Fig. 6.** Flexural strengths from experiments and FEA predictions.

ratio of 32 was chosen and five specimens were tested for each stacking sequence. The crosshead speed was chosen to be 0.5 mm/min. The loads and displacements were recorded and the flexural modulus and strength were calculated using Eqs. (2) and (3). The same stacking sequences were modelled by the FEA based model.

For stacking sequence $[0_G/0_{3C}]_S$, the initial failure occurs when the displacement is around 6 mm. At this displacement, the stresses of ply 1 and ply 8 from FEA are shown in Fig. 3, from which it is seen that ply 1 is in tension and ply 8 is in compression. The maximum failure criteria of ply 1 and ply 8 from FEA are shown in Fig. 4. A value greater than or equal to 1 means failure has occurred. It is seen that failure initiates at ply 8, which is on the compressive face.

The stress-strain curve of $[0_G/0_{3C}]_S$ from FEA is shown in Fig. 5. The maximum failure criteria are also plotted, from which the failure point can be determined. The number of sub-steps was automatically chosen by Ansys.

The flexural strengths from the experiments and model predictions are shown in Fig. 6. It is shown from Fig. 6 that the FEA predictions and experimental results are in good agreement. The full carbon composite has the highest flexural strength. However, some hybrid stacking sequences e.g. $[0_{2G}/0_{2C}]_S$ show promising flexural strengths.

The FEA based approach was further validated against the experimental data in [1]. The flexural strengths and moduli are shown in Fig. 7. For most stacking sequences, the FEA and experimental results are in good agreement, with the exception of $[CG_2CG]_S$ composite, of which the flexural strength is much higher than the FEA prediction. In the hybrid composite of $[CG_2CG]_S$ type, the distribution of glass and carbon fibre layers are balanced. The deformation of carbon fibre layers is bridged by more ductile glass fibre layers adjacent to it, resulting in the highest flexural strength [13].

### 2.4. Model application

Composite specimens consisted of 8 unidirectional fibre reinforced plies were simulated by the developed model. The thickness of each ply is 0.25 mm. In addition to the five stacking sequences as shown in Fig. 2, three additional hybrid stacking sequences $[0_C/0_{3G}]_S$, $[0_{2C}/0_{2G}]_S$ and $[0_{3C}/0_G]_S$ were simulated. The fibre volume fractions of the carbon and glass fibre plies were chosen to be 30% and 50%, respectively. The fibre volume fractions were chosen so that the full carbon and full glass fibre composites had similar flexural strengths. The fibre volume fractions of the carbon and glass fibre plies were then increased to 40% and 60%, respectively, and simulation was repeated. Furthermore, the flex-

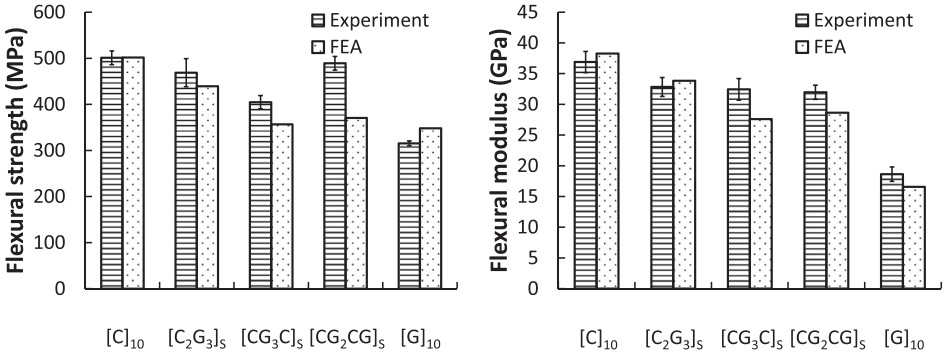


**Fig. 7.** Flexural strengths (left) and moduli (right) of various stacking sequences.

**Table 2**
Variables and their ranges of value in optimisation.

| Variable | Range of value |
|---|---|
| $V_{fc}$ | [0.3, 0.6] |
| $V_{fg}$ | [0.3, 0.6] |
| Ply material | [Carbon/epoxy, glass/epoxy] |

**Table 3**
Failure sequences of various stacking sequences when the fibre volume fractions of the carbon/epoxy and glass/epoxy plies are 30% and 50% respectively.

| Stacking sequence | Failure sequence (first to last) | | | | | | | | Failure initiates |
|---|---|---|---|---|---|---|---|---|---|
| $[0]_{8C}$ | 8 | 7 | 6 | 5 | 4 | 1 | 3 | 2 | Carbon fibre plies |
| $[0_G/0_{3C}]_S$ | 7 | 6 | 8 | 5 | 4 | 3 | 1 | 2 | Carbon fibre plies |
| $[0_{3C}/0_C]_S$ | 8 | 7 | 6 | 5 | 4 | 1 | 2 | 3 | Carbon fibre plies |
| $[0_{2G}/0_{2C}]_S$ | 8 | 6 | 7 | 5 | 4 | 3 | 1 | 2 | Glass fibre plies |
| $[0_{2C}/0_{2G}]_S$ | 8 | 7 | 6 | 5 | 4 | 1 | 2 | 3 | Carbon fibre plies |
| $[0_{3G}/0_C]_S$ | 8 | 7 | 6 | 5 | 4 | 3 | 1 | 2 | Glass fibre plies |
| $[0_C/0_{3G}]_S$ | 8 | 7 | 6 | 5 | 4 | 1 | 3 | 2 | Carbon fibre plies |
| $[0]_{8G}$ | 8 | 7 | 6 | 5 | 4 | 3 | 2 | 2 | Glass fibre plies |

ural performance was simulated when the fibre volume fractions of the carbon/epoxy and glass/epoxy plies are both 50%. Lastly, the simulation was conducted when the fibre volume fractions of the carbon and glass fibre plies were 50% and 30%, respectively.

### 2.5. Optimisation

The FEA based model was coupled with MOGA [24,25] to conduct optimisation with two objectives of minimising the cost and weight, and a constraint of required flexural strength. The areal cost of hybrid composites is given by

$$C_c = \sum_{i=1}^{8} \left[C_{fi} V_{fi} + C_m (1 - V_{fi})\right] \tag{4}$$

where $C_c$, $C_f$ and $C_m$ are the areal costs of the composite, the fibre and the matrix respectively.

The areal density of hybrid composites is given by

$$\rho_c = \sum_{i=1}^{8} \left[\rho_{fi} V_{fi} + \rho_m (1 - V_{fi})\right] \tag{5}$$

where $\rho_c$, $\rho_f$ and $\rho_m$ are the areal densities of the composite, the fibre and the matrix respectively.

The design variables were the fibre type of each ply, and the fibre volume fraction carbon/epoxy and glass/epoxy laminas. The variables and their ranges of value are shown in Table 2.

## 3. Results and discussion

When the fibre volume fractions of the carbon/epoxy and glass/epoxy plies are 30% and 50% respectively, the flexural strengths and moduli of various stacking sequences are shown in Fig. 8. It is seen the flexural strength increases when glass/epoxy plies are placed on the outside of the hybrid composite. The hybrid composites has the highest flexural strength when it contains half carbon/epoxy plies and half glass/epoxy plies. It is shown positive hybrid effects exist in this case. This is in consistency with our previous research [5,6,10,11]. Conversely, placing glass/epoxy plies at the inside of the hybrid composite decreases the flexural strength. With reference to the full carbon fibre composite, when carbon/epoxy plies are replaced by glass/epoxy plies from the outside, the flexural modulus decreases rapidly towards the full glass fibre composite. On the other hand, when the replacement occurs at the inside of the composite, the flexural modulus decrease slowly. This is because the full carbon composite has a higher flexural modulus than the full glass composite, so that placing carbon/epoxy plies on the outside of the hybrid composite will maintain the stiffness.

The failure sequences of various stacking sequences being studied are summarised in Table 3. It is noticed that for most stacking sequences, failure initiates at the topmost ply. The only exception is $[0_G/0_{3C}]_S$, in which failure initiates at the second topmost ply, followed by the third topmost ply.

When the fibre volume fractions of the carbon/epoxy and glass/epoxy plies are 40% and 60% respectively, simulation was repeated for the same stacking sequences. The flexural strengths and moduli of various stacking sequences are shown in Fig. 9. It is also seen the flexural strength increases when glass/epoxy plies are placed on the outside of the hybrid composite. The hybrid composites has the highest flexural strength when it contains half carbon/epoxy plies and half glass/epoxy plies. The flexural moduli show similar trends as shown in Fig. 8.

When the fibre volume fractions of the carbon/epoxy and glass/epoxy plies are both 50%, the flexural strengths and moduli are shown in Fig. 10. It is show that when the carbon/epoxy plies are placed on the outside of the hybrid composite, the hybrid composite has comparable flexural strength and modulus as the full carbon composite when up to half of the plies are glass/epoxy. It is also noticed that the full carbon composite has a higher flexural strength compared to the aforementioned results because it contains more carbon fibre. This suggests that the cost of composites can be significantly reduced via hybridisation while maintaining the minimum required flexural strength. However, because the glass fibre has a much higher density than the carbon fibre, the fibre volume fraction of the glass/epoxy plies should be low for the purpose of reducing the weight. The flexural moduli show similar trends as shown in Fig. 8.

When the fibre volume fractions of the carbon/epoxy and glass/epoxy plies are 50% and 30%, respectively, the flexural strengths and moduli are shown in Fig. 11. It is show that when the carbon/epoxy

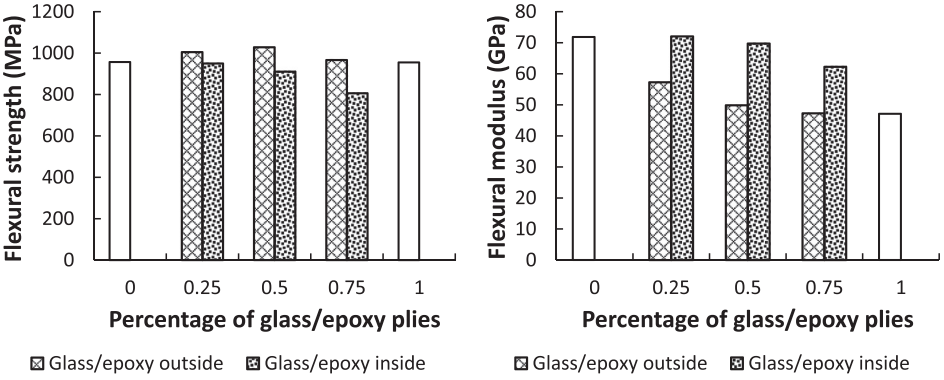


**Fig. 8.** Flexural strengths (left) and moduli (right) of various stacking sequences when the fibre volume fractions of the carbon/epoxy and glass/epoxy plies are 30% and 50% respectively.

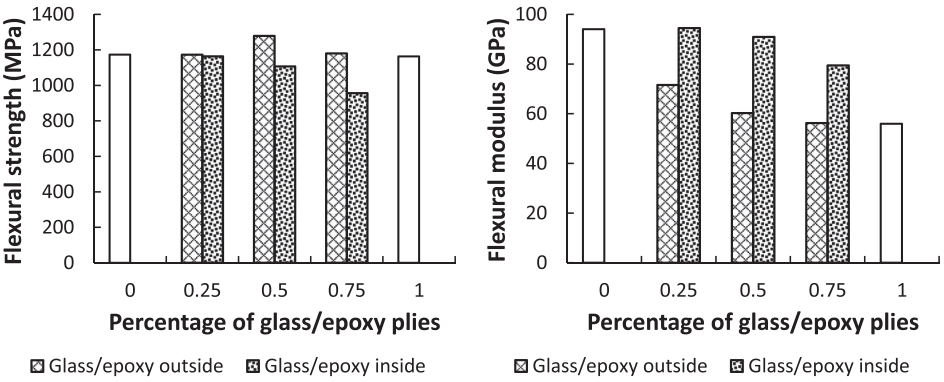


**Fig. 9.** Flexural strengths (left) and moduli (right) of various stacking sequences when the fibre volume fractions of the carbon/epoxy and glass/epoxy plies are 40% and 60% respectively.

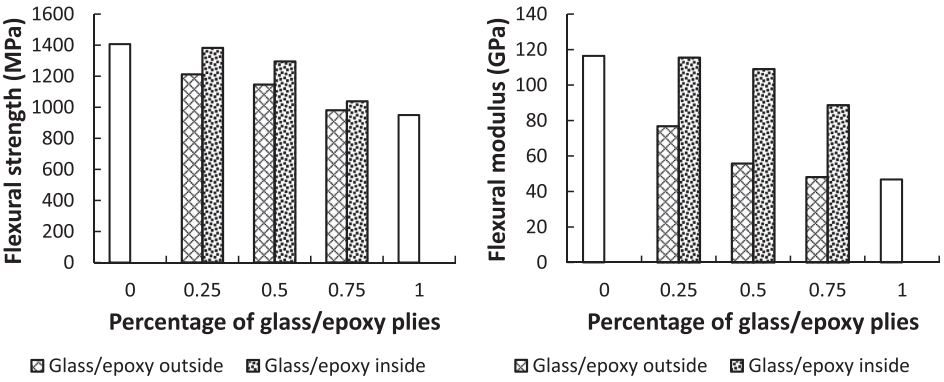


**Fig. 10.** Flexural strengths (left) and moduli (right) of various stacking sequences when the fibre volume fractions of the carbon/epoxy and glass/epoxy plies are both 50%.

plies are placed on the outside of the hybrid composite, the hybrid composite has comparable flexural strength and modulus as the full carbon composite when up to half of the plies are glass/epoxy. However, when the glass/epoxy plies are placed on the outside of the hybrid composite, the flexural strength is reduced significantly compared to the full carbon composite. This suggests that it is possible to achieve optimal design when both the cost and weight are of concern subjected to the minimum required flexural strength. Likewise, similar trends as shown in Fig. 8 are shown for the flexural modulus.

When the fibre volume fractions of the carbon/epoxy and glass/epoxy plies are 50% and 30% respectively, the failure sequences of various stacking sequences being studied are summarised in Table 4. Compared to Table 3, it is shown that similar failure sequences occur for most stacking sequences, and failure initiates at the topmost ply (compressive face). The only exception is $[0_G/0_{3C}]_S$, in which failure initiates at the second topmost ply, followed by the topmost ply.

The Pareto fronts from MOGA optimisation when the constraint flexural strength is 1300 MPa is shown in Fig. 12, in which the two conflicting objectives: cost and weight are plotted.

**Table 4**
Failure sequences of various stacking sequences when the fibre volume fractions of the carbon/epoxy and glass/epoxy plies are 50% and 30% respectively.

| Stacking sequence | Failure sequence (first to last) | | | | | | | | Failure initiates |
|---|---|---|---|---|---|---|---|---|---|
| $[0]_{8C}$ | 8 | 7 | 6 | 5 | 4 | 1 | 3 | 2 | Carbon fibre plies |
| $[0_G/0_{3C}]_S$ | 7 | 8 | 6 | 5 | 4 | 3 | 2 | 1 | Carbon fibre plies |
| $[0_{3C}/0_G]_S$ | 8 | 7 | 6 | 5 | 4 | 3 | 1 | 2 | Carbon fibre plies |
| $[0_{2G}/0_{2C}]_S$ | 8 | 6 | 7 | 5 | 4 | 1 | 2 | 3 | Glass fibre plies |
| $[0_{2C}/0_{2G}]_S$ | 8 | 7 | 6 | 5 | 4 | 1 | 3 | 2 | Carbon fibre plies |
| $[0_{3G}/0_C]_S$ | 8 | 7 | 5 | 6 | 4 | 1 | 2 | 3 | Glass fibre plies |
| $[0_C/0_{3G}]_S$ | 8 | 7 | 6 | 5 | 4 | 3 | 1 | 2 | Carbon fibre plies |
| $[0]_{8G}$ | 8 | 7 | 6 | 5 | 4 | 1 | 3 | 2 | Glass fibre plies |

The optimal candidates are shown in Table 5, from which it is shown that the dominant optimal stacking sequence is $[0]_{8C}$ or $[0_{3C}/0_G]_S$. This confirms the aforementioned finding that when the carbon/epoxy plies are placed on the outside of the hybrid composite, the hybrid composite has comparable flexural strength and modulus as the full carbon composite when up to half of the plies are glass/epoxy. Since the glass fibre

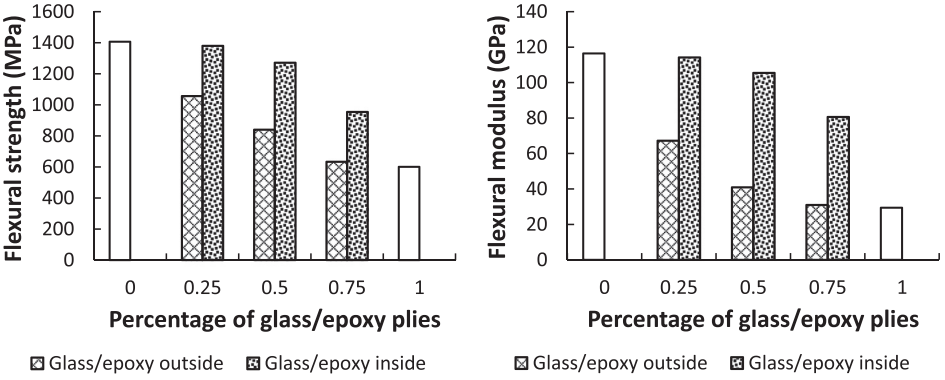


**Fig. 11.** Flexural strengths (left) and moduli (right) of various stacking sequences when the fibre volume fractions of the carbon/epoxy and glass/epoxy plies are 50% and 30% respectively.

**Table 5**
Optimal candidates when the required flexural strength is 1300 MPa.

| Candidate | $V_{fc}$ (%) | $V_{fg}$ (%) | Stacking sequence | Cost ($/m$^2$) | Weight (mg/mm$^3$) | Flexural strength (MPa) |
|---|---|---|---|---|---|---|
| 1 | 51.90 | 33.85 | $[0_{2C}/0_{2G}]_S$ | 143.38 | 3.0123 | 1317 |
| 2 | 48.36 | 33.85 | $[0_{3C}/0_G]_S$ | 156.13 | 2.9270 | 1351 |
| 3 | 47.05 | – | $[0]_{8C}$ | 170.02 | 2.8481 | 1336 |
| 4 | 47.11 | – | $[0]_{8C}$ | 170.17 | 2.8489 | 1337 |
| 5 | 47.22 | – | $[0]_{8C}$ | 170.45 | 2.8505 | 1340 |
| 6 | 52.02 | 32.83 | $[0_{3C}/0_G]_S$ | 162.60 | 2.9589 | 1439 |
| 7 | 52.05 | 32.84 | $[0_{3C}/0_G]_S$ | 162.65 | 2.9592 | 1440 |
| 8 | 52.07 | 32.83 | $[0_{3C}/0_G]_S$ | 162.69 | 2.9594 | 1440 |
| 9 | 47.30 | – | $[0]_{8C}$ | 170.65 | 2.8517 | 1342 |

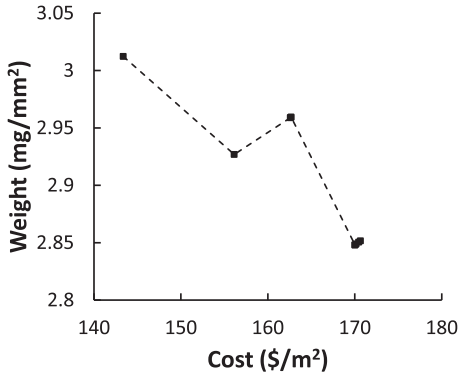


**Fig. 12.** Pareto front when the required flexural strength is 1300 MPa.

has a much higher density than the carbon fibre, the optimal results tend to keep the fibre volume fraction of the glass/epoxy plies low.

## 4. Conclusions

In this study, the flexural properties of symmetric carbon and glass fibre reinforced hybrid composite laminates was investigated both experimentally and numerically. It is shown from both the experiments and FEA predictions that the flexural strength can be improved via hybridisation. When the full carbon and full glass composites have similar flexural strengths, the glass/epoxy plies should be placed on the outside of the hybrid composite in order to obtain positive hybrid effects. The highest flexural strength is achieved when the hybrid composite contains half carbon/epoxy plies and half glass/epoxy plies. When the full carbon composite has a higher flexural strength than the full glass composite, the stiffer plies, i.e. carbon/epoxy plies should be placed on the outside of the hybrid composite in order to maintain its stiffness. The hybrid composite has comparable flexural strength and modulus as the full carbon composite when up to half of the plies are glass/epoxy and placed on the inside of the composite. From this perspective, optimisation can be done with the cost and weight being the objectives subjected to a given flexural strength.

## Declaration of Competing Interest

There is no conflict of interest.

## References

[1] D.K. Jesthi, R.K. Nayak, Evaluation of mechanical properties and morphology of seawater aged carbon and glass fiber reinforced polymer hybrid composites, Compos. Part B 174 (2019) 106980.
[2] T.A. Sebaey, A. Wagih, Flexural properties of notched carbon-aramid hybrid composite laminates, J. Compos. Mater. 53 (28–30) (2019) 4137–4148.
[3] A. Wagih, et al., Post-impact flexural behavior of carbon-aramid/epoxy hybrid composites, Compos. Struct. 239 (2020) 112022.
[4] S. Fischer, G. Marom, The flexural behaviour of aramid fibre hybrid composite materials, Compos. Sci. Technol. 28 (4) (1987) 291–314.
[5] C. Dong, H.A. Ranaweera-Jayawardena, I.J. Davies, Flexural properties of hybrid composites reinforced by S-2 glass and T700S carbon fibres, Compos. Part B 43 (2) (2012) 573–581.
[6] C. Dong, J. Duong, I.J. Davies, Flexural properties of S-2 glass and TR30S carbon fiber-reinforced epoxy hybrid composites, Polym. Compos. 33 (5) (2012) 773–781.
[7] C. Dong, I.J. Davies, Flexural properties of glass and carbon fiber reinforced epoxy hybrid composites, Proc. Inst. Mech. Eng. Part L 227 (4) (2013) 308–317.
[8] C. Dong, Sudarisman, I.J. Davies, Flexural properties of E glass and TR50S carbon fiber reinforced epoxy hybrid composites, J. Mater. Eng. Perform. 22 (1) (2013) 41–49.
[9] P.W. Manders, M.G. Bader, The strength of hybrid glass/carbon fibre composites, J. Mater. Sci. 16 (8) (1981) 2233–2245.
[10] C. Dong, I.J. Davies, Optimal design for the flexural behaviour of glass and carbon fibre reinforced polymer hybrid composites, Mater. Des. 37 (2012) 450–457.
[11] C. Dong, I.J. Davies, Flexural and tensile strengths of unidirectional hybrid epoxy composites reinforced by S-2 glass and T700S carbon fibres, Mater. Des. 54 (2014) 955–966.
[12] M. Jalalvand, G. Czél, M.R. Wisnom, Numerical modelling of the damage modes in UD thin carbon/glass hybrid laminates, Compos. Sci. Technol. 94 (2014) 39–47.
[13] J. Zhang, et al., Hybrid composite laminates reinforced with glass/carbon woven fabrics for lightweight load bearing structures, Mater. Des. 36 (2012) 75–80.
[14] T.-W. Chou, Microstructural Design of Fiber Composites, Cambridge University Press, Cambridge, U.K, 1992.
[15] Z. Hashin, Analysis of composite materials—a survey, J. Appl. Mech. 50 (3) (1983) 481–505.
[16] M. Kalantari, C. Dong, I.J. Davies, Multi-objective analysis for optimal and robust design of unidirectional glass/carbon fibre reinforced hybrid epoxy composites under flexural loading, Compos. Part B 84 (2016) 130–139.

[17] I.D.G. Ary Subagia, et al., Effect of stacking sequence on the flexural properties of hybrid composites reinforced with carbon and basalt fibers, Compos. Part B 58 (2014) 251–258.
[18] K.S. Pandya, C. Veerraju, N.K. Naik, Hybrid composites made of carbon and glass woven fabrics under quasi-static loading, Mater. Des. 32 (7) (2011) 4094–4099.
[19] S.H. Lee, A.M. Waas, Compressive response and failure of fibre reinforced unidirectional composites, Int. J. Fract. 100 (3) (1999) 275–306.
[20] K.H. Lo, E.S.M. Chim, Compressive strength of unidirectional composites, J. Reinforced Plast. Compos. 11 (8) (1992) 838–896.
[21] B. Budiansky, N.A. Fleck, Compressive failure of fibre composites, J. Mech. Phys. Solids 41 (1) (1993) 183–211.
[22] R.E. Bullock, Strength ratios of composite materials in flexure and in tension, J. Compos. Mater. 8 (1974) 200–206.
[23] ASTM International, Standard test method for flexural properties of polymer matrix composite materials, ASTM D7264/D7264M-15, ASTM International, West Conshohocken, PA, USA, 2015.
[24] M. Kalantari, C. Dong, I.J. Davies, Multi-objective robust optimisation of unidirectional carbon/glass fibre reinforced hybrid composites under flexural loading, Compos. Struct. 138 (2016) 264–275.
[25] M. Kalantari, C. Dong, I.J. Davies, Multi-objective robust optimization of multi-directional carbon/glass fibre-reinforced hybrid composites with manufacture related uncertainties under flexural loading, Compos. Struct. 182 (2017) 132–142.